Thermal Analysis of Antenna Structures Part II – Panel Temperature Distribution

D. Schonfeld and F. L. Lansing
Ground Antennas and Facilities Engineering Section

This article is the second in a series that analyzes the temperature distribution in microwave antennas. An analytical solution in a series form is obtained for the temperature distribution in a flat plate analogous to an antenna surface panel under arbitrary temperature and boundary conditions. The solution includes the effects of radiation and air convection from the plate. Good agreement is obtained between the numerical and analytical solutions.

I. Introduction

In a previous article (Ref. 1) we have indicated that construction requirements for large Ka-band antennas are more stringent than those presently used for the S- or X-bands. In particular, for the Ka-band antennas, environmental factors such as temperature variations can have deleterious effects on the antenna panels setting, alignment, antenna pointing and tracking and therefore on the antenna performance.

In Ref. 1 we have presented a method of analysis that was used for thermal modeling of the links which make up the antenna's backup structure. The present article extends the thermal modeling by considering the antenna surface panels. In future articles we will tie the present panel temperature analysis to the thermal analysis of the backup structure. In this way we aim to obtain a temperature simulation of the complete antenna structure and, from this, calculate the thermal stresses in the antenna members.

II. Analysis

To model a single antenna panel, we will be considering a two-dimensional rectangular plate of length a and width b as shown in Fig. 1. The two-dimensional assumption is warranted because the thickness of the antenna panel is much smaller than the other dimensions. We want to find the temperature distribution and the heat flux in this plate under the following assumptions:

(1) Arbitrary, steady-state temperature boundary conditions; these are labeled $T_N(x)$, $T_E(y)$, $T_S(x)$, and $T_W(y)$ in Fig. 1. for the north, east, south and west sides of the rectangle, respectively.

(2) Heat transfer in the plate occurs due to conduction, air convection and solar and IR radiation. The plate is characterized by a thermal conductivity k, a convection coefficient h_c and a short wave solar absorptivity α. No internal heat generation is assumed.

(3) Linearized approximation for the radiation heat transfer to ambient term as indicated in Ref. 1 results in a radiative heat transfer coefficient

$$h_r = \epsilon \sigma \mathsf{F} (T^2 + T_a^2)(T + T_a)$$

Under these conditions, the two-dimensional heat transfer equation is

$$\frac{\partial^2 T}{\partial x^2} + \frac{\partial^2 T}{\partial y^2} = \left(\frac{h_r + h_c}{k}\right) T + \left(\frac{\alpha I}{k} - \frac{h_r + h_c}{k} T_a\right) \quad (1)$$

or

$$\nabla^2 T = a_1 T + a_2 \quad (2)$$

where

$$a_1 = \frac{h_r + h_c}{k}$$

$$a_2 = \frac{\alpha I}{k} - \frac{h_r + h_c}{k} T_a \quad (3)$$

Equation (2) is a nonhomogeneous partial differential equation. The following nonhomogeneous boundary conditions are formed for Eq. (1):

$$\begin{aligned} T &= T_W(y) \quad \text{for } x = 0, \\ T &= T_E(y) \quad \text{for } x = a, \\ T &= T_S(x) \quad \text{for } y = 0, \\ T &= T_N(x) \quad \text{for } y = b. \end{aligned} \quad (4)$$

The following cases are studied to verify the accuracy limits between analytical solutions in series form and numerical solutions for homogeneous and nonhomogeneous forms of the equation.

Case 1. Simple Conduction Problem – Series Solution

When $a_1 = a_2 = 0$, Eq. (2) reduces to the conventional Laplace's equation and represents a two-dimensional temperature distribution due to conduction heat transfer only (Ref. 2). For this simplified case one obtains the following series solution.

$$\begin{aligned} T(x,y) &= \frac{2}{a} \sum_{m=1}^{\infty} \frac{\int_0^a T_N(x) \sin \frac{m\pi x}{a} dx}{\sinh m\pi} \sin \frac{m\pi x}{a} \sinh \frac{m\pi y}{b} \\ &+ \frac{2}{a} \sum_{m=1}^{\infty} \frac{\int_0^a T_S(x) \sin \frac{m\pi x}{a} dx}{\sinh (-m\pi)} \sin \frac{m\pi x}{a} \sinh \frac{m\pi(y-b)}{b} \\ &+ \frac{2}{b} \sum_{m=1}^{\infty} \frac{\int_0^b T_E(y) \sin \frac{m\pi y}{b} dy}{\sinh m\pi} \sin \frac{m\pi y}{b} \sinh \frac{m\pi x}{a} \\ &+ \frac{2}{b} \sum_{m=1}^{\infty} \frac{\int_0^b T_W(y) \sin \frac{m\pi y}{b} dy}{\sinh (-m\pi)} \sin \frac{m\pi y}{b} \sinh \frac{m\pi(x-a)}{a} \end{aligned} \quad (5)$$

If one expands the temperature boundary conditions T_N, T_S, T_E and T_W in uniformly convergent Fourier series, the temperature distribution $T(X, Y)$ will no longer involve integrals. For this case, the solution is given in Ref. 2.

Case 2. Simple Conduction Problem–Numerical Solutions

The series solution, Eq. (5), can be truncated, and computed numerically for any arbitrary but finite number of terms. In this computation, as the number of terms and the arguments of the trigonometric functions become large, numerical errors can accumulate and cause instability. Therefore, when the computational programs were run on JPL's UNIVAC 1181, double precision was used for all the variables. The results of numerically computing the truncated series solution can be compared with those obtained by solving Laplace's equation by numerical means (Ref. 3). The two methods should give agreeable answers and thus serve as a check on each other. As an example, consider a square flat plate ($a = b = 1$) where the temperature boundary conditions (nonhomogeneous) are given by:

$$\begin{aligned} T_N(x) &= 150x + 50 \\ T_E(x) &= 100y + 100 \\ T_S(x) &= -200x + 300 \\ T_W(y) &= -250y + 300 \\ &(0 < x < 1, 0 < y < 1) \end{aligned} \quad (6)$$

The resulting isotherms for this case are illustrated in Fig. 2. The series computation from Eq. (5) is truncated at the tenth term ($m = 10$) and the results show good agreement with those obtained by a numerical solution of Laplace's equation (results are listed in Table 1).

Case 3. The Nonhomogeneous Case—Series Solution

Where a_1 and a_2 are both nonzero, Eqs. (2) and (4) form a complex nonhomogeneous boundary value problem with nonhomogeneous differential equation and nonhomogeneous boundary conditions. However, taking advantage of linearity we use superposition to solve the nonhomogeneous boundary conditions and separation of variables to solve the nonhomogeneous differential equation as follows.

Let $T(x, y)$ be expressed as a sum of two functions:

$$T(x, y) = u(x, y) + f(a_1, a_2) \tag{7}$$

If the constant $f(a_1, a_2)$ is chosen such that:

$$f(a_1, a_2) = -\frac{a_2}{a_1} \tag{8}$$

then replacing (7) into (2) results in a homogeneous partial differential equation in $u(x, y)$:

$$\nabla^2 u(x, y) = a_1 u(x, y) \tag{9}$$

with the following four nonhomogeneous boundary conditions

$$\begin{aligned} u(x,0) &= T_X(x) + \frac{a_2}{a_1} \\ u(x,b) &= T_N(x) + \frac{a_2}{a_1} \\ u(a,y) &= T_W(y) + \frac{a_2}{a_1} \\ u(a,y) &= T_E(y) + \frac{a_2}{a_1} \end{aligned} \tag{10}$$

The linearity of Eq. (9) allows us to use superposition of four subproblems; each one has a single nonhomogeneous boundary condition. Write $u(x, y)$ as the sum

$$u(x, y) = s(x, y) + t(x, y) + v(x, y) + w(x, y) \tag{11}$$

which when inserted into (9) and (10) gives the following:

$$\nabla^2 s(x,y) + \nabla^2 t(x,y) + \nabla^2 v(x,y) + \nabla^2 w(x,y) = a_1 s(x, y) + a_1 t(x, y) + a_1 v(x, y) + a_1 w(x, y) \tag{12}$$

with the following four boundary conditions:

$$\begin{aligned} s(x,0) + t(x,0) + v(x,0) + w(x,0) &= T_S(x) + \frac{a_2}{a_1} \\ s(x,b) + t(x,b) + v(x,b) + w(x,b) &= T_N(x) + \frac{a_2}{a_1} \\ s(0,y) + t(0,y) + v(0,y) + w(0,y) &= T_W(y) + \frac{a_2}{a_1} \\ s(a,y) + t(a,y) + v(a,y) + w(a,y) &= T_E(y) + \frac{a_2}{a_1} \end{aligned} \tag{13}$$

Therefore, the solution of homogeneous Eq. (9) with nonhomogeneous boundary conditions (10) can be obtained by solving four subproblems each one having at most one nonhomogeneity. These four subproblems are

Subproblem 1: $\Delta^2 s = a_1 s$

$$\begin{aligned} \nabla s(x,0) &= T_S(x) + \frac{a_2}{a_1} \\ s(x,b) &= 0 \\ s(o,y) &= 0 \\ s(a,y) &= 0 \end{aligned} \tag{14}$$

Subproblem 2: $\nabla^2 t = a_1 t$

$$\begin{aligned} t(x,0) &= 0 \\ t(x,b) &= T_N(x) + \frac{a_2}{a_1} \\ t(o,y) &= 0 \\ t(a,y) &= 0 \end{aligned} \tag{15}$$

Subproblem 3: $\nabla^2 v = a_1 v$

$$v(x,0) = 0$$

$$v(x,b) = 0 \tag{16}$$

$$v(0,y) = T_W(y) + \frac{a_2}{a_1}$$

$$v(a,y) = 0$$

Subproblem 4: $\nabla^2 w = a_1 w$

$$w(x,0) = 0$$

$$w(x,b) = 0 \tag{17}$$

$$w(0,y) = 0$$

$$w(a,y) = T_E(y) + \frac{a_2}{a_1}$$

The solution to subproblem 1 can be found in Ref. 4 as

$$s(x,y) = \frac{2}{a} \sum_{m=1}^{\infty} \frac{\sin \bar{x}_m \sinh((b-y)\gamma_m)}{\sinh b\gamma_m} \int_0^a \left[T_S(x) + \frac{a_2}{a_1}\right] \sin \bar{x}_m \, dx \tag{18}$$

where

$$\bar{x}_m = \frac{m\pi x}{a} \tag{19}$$

$$\gamma_m = \left(a_1 + \frac{m^2\pi^2}{a^2}\right)^{1/2} \tag{20}$$

By analogy with Eq. (18), the other subproblems have the following solutions.

For subproblem 2, the solution is:

$$t(x,y) = \frac{2}{a} \sum_{m=1}^{\infty} \frac{\sin \bar{x}_m \sinh(y\gamma_m)}{\sinh b\gamma_m} \int_0^a \left[T_N(x) + \frac{a_2}{a_1}\right] \sin \bar{x}_m \, dx \tag{21}$$

For subproblem 3, the solution is:

$$v(x,y) = \frac{2}{b} \sum_{m=1}^{\infty} \frac{\sin \bar{y}_m \sinh((a-x)\eta_m)}{\sinh a\eta_m} \int_0^b \left[T_W(y) + \frac{a_2}{a_1}\right] \sin \bar{y}_m \, dy \tag{22}$$

For subproblem 4, the solution is:

$$w(x,y) = \frac{2}{b} \sum_{m=1}^{\infty} \frac{\sin \bar{y}_m \sinh(x\eta_m)}{\sinh a\eta_m} \int_0^b \left[T_E(y) + \frac{a_2}{a_1}\right] \sin \bar{y}_m \, dy \tag{23}$$

where

$$\bar{y}_m = \frac{m\pi y}{a} \tag{24}$$

$$\eta_m = \left(a_1 + \frac{m^2\pi^2}{b^2}\right)^{1/2} \tag{25}$$

Therefore, the actual temperature field, $T(x,y)$, from Eq. (7) is given by adding Eqs. (18), (21), (22) and (23)

$$\begin{aligned} T(x,y) = {} & \frac{2}{a} \sum_{m=1}^{\infty} \frac{\sin \bar{x}_m \sinh((b-y)\gamma_m}{\sinh b\gamma_m} \int_0^a \left[T_S(x) + \frac{a_2}{a_1}\right] \sin \bar{x}_m \, dx \\ & + \frac{2}{a} \sum_{m=1}^{\infty} \frac{\sin \bar{x}_m \sinh(y\gamma_m)}{\sinh b\gamma_m} \int_0^a \left[T_N(x) + \frac{a_2}{a_1}\right] \sin \bar{x}_m \, dx \\ & + \frac{2}{b} \sum_{m=1}^{\infty} \frac{\sin \bar{y}_m \sinh((a-x)\eta_m)}{\sinh a\eta_m} \int_0^b \left[T_W(y) + \frac{a_2}{a_1}\right] \sin \bar{y}_m \, dy \\ & + \frac{2}{b} \sum_{m=1}^{\infty} \frac{\sin \bar{y}_m \sinh(x\eta_m)}{\sinh a\eta_m} \int_0^b \left[T_E(y) + \frac{a_2}{a_1}\right] \sin \bar{y}_m \, dy \\ & - \frac{a_2}{a_1} \end{aligned} \tag{26}$$

Equation (26) describes the temperature field throughout the plate, except at the corner points. For example, for the boundary $x = 0$, Eq. (26) reduces to

$$T(0,y) = \frac{2}{b} \sum_{m=1}^{\infty} \sin \bar{y}_m \int_0^b \left[T_W(y) + \frac{a_2}{a_1} \right] \sin \bar{y}_m \, dy - \frac{a_2}{a_1} \tag{27}$$

If $T_W(y)$ is constant, Eq. (27) further simplifies to

$$T(0,y) = 2 \left(T_W + \frac{a_2}{a_1} \right) \sum_{m=1}^{\infty} \sin y_m \frac{(1 - \cos m\pi)}{m\pi} - \frac{a_2}{a_1} = T_W \tag{28}$$

and the sum

$$\sum_{m=1}^{\infty} \sin \bar{y}_m \frac{(1 - \cos m\pi)}{m\pi}$$

can be evaluated numerically. The series converges to a value of 0.5 but the convergence is quite slow, as shown in Fig. 3, where after 200 terms, the value of the series is 0.498. The series converges to a value of 0.5 even close to the plate corners, but the closer one approaches these corners, the slower the convergence is (see Fig. 4).

Our model of the antenna surface panels and their backup structure assumes that the bars placed at the edges of each panel receive heat from the panels by conduction only. This means that we must calculate the heat flux ϕ at each edge, where

$$\phi_z = \frac{\partial T}{\partial x} + \frac{\partial T}{\partial y} \tag{29}$$

Using Eq. (26) and Leibnitz's rule, these edge fluxes are calculated as follows:

$$\phi_{y=0} = \frac{2}{a} \left[\sum_{m=1}^{\infty} \frac{m\pi}{a} \left\{ \sin \bar{x}_m \int_0^a \bar{T}_S \cos \bar{x}_m \, dx + \cos \bar{x}_m \int_0^a \bar{T}_S \sin \bar{x}_m \, dx \right\} + \sin \bar{x}_m \int_0^a \sin \bar{x}_m \frac{\partial \bar{T}_S}{\partial x} dx \right]$$

$$+ \frac{2}{a} \left[\sum_{m=1}^{\infty} \frac{-\gamma_m \sin \bar{x}_m}{\tanh b\gamma_m} \int_0^a \bar{T}_S \sin \bar{x}_m \, dx \right]$$

$$+ \frac{2}{a} \left[\sum_{m=1}^{\infty} \frac{\gamma_m \sin \bar{x}_m}{\sinh b\gamma_m} \int_0^a \bar{T}_N \sin \bar{x}_m \, dx \right]$$

$$+ \frac{2}{b} \left[\sum_{m=1}^{\infty} \frac{m\pi}{b} \frac{\sinh((a - x_m)\eta_m)}{\sinh a\eta_m} \int_0^b \bar{T}_W \sin \bar{y}_m \, dy \right]$$

$$+ \frac{2}{b} \left[\sum_{m=1}^{\infty} \frac{m\pi}{b} \frac{\sinh x\eta_m}{\sinh a\eta_m} \int_0^b \bar{T}_E \sin \bar{y}_m \, dy \right] \tag{30}$$

$$\phi_{y=b} = \frac{2}{a} \left[\sum_{m=1}^{\infty} \frac{m\pi}{a} \left\{ \sin \bar{x}_m \int_0^a \bar{T}_N \cos \bar{x}_m \, dx + \cos \bar{x}_m \int_0^a \bar{T}_N \sin \bar{x}_m \, dx \right\} + \sin \bar{x}_m \int_0^a \sin \bar{x}_m \frac{\partial \bar{T}_N}{\partial x} dx \right]$$

$$+ \frac{2}{a} \left[\sum_{m=1}^{\infty} \frac{\gamma_m \sin \bar{x}_m}{\tanh b\gamma_m} \int \bar{T}_N \sin \bar{x}_m \, dx \right]$$

$$+ \frac{2}{a} \left[\sum_{m=1}^{\infty} \frac{-\gamma_m \sin \bar{x}_m}{\sinh b\gamma_m} \int \bar{T}_S \sin \bar{x}_m \, dx \right]$$

$$+ \frac{2}{b} \left[\sum_{m=1}^{\infty} \frac{m\pi}{b} \frac{\sinh((a - x)\eta_m)}{\sinh a\eta_m} (-1)^m \int \bar{T}_W \sin y_m \, dy \right]$$

$$+ \frac{2}{b} \left[\sum_{m=1}^{\infty} \frac{m\pi}{b} \frac{\sinh x\eta_m}{\sinh a\eta_m} (-1)^m \int \bar{T}_E \sin \bar{y}_m \, dy \right] \tag{31}$$

$$\phi_{x=0} = \frac{2}{b} \left[\sum_{m=1}^{\infty} \frac{m\pi}{b} \left\{ \sin \bar{y}_m \int_0^b \bar{T}_W \cos \bar{y}_m \, dy + \cos \bar{y}_m \int_0^b \bar{T}_W \sin \bar{y}_m \, dy \right\} \right.$$

$$+ \sin \bar{y}_m \int_0^b \sin \bar{y}_m \frac{\partial \bar{T}_W}{\partial y} dy \Bigg]$$

$$+ \frac{2}{b} \left[\sum_{m=1}^{\infty} \frac{-\eta_m \sin \bar{y}_m}{\tanh a\eta_m} \int_0^b \bar{T}_W \sin \bar{y}_m \, dy \right]$$

$$+ \frac{2}{b} \left[\sum_{m=1}^{\infty} \frac{\eta_m \sin \bar{y}_m}{\sinh a\eta_m} \int_0^b \bar{T}_E \sin \bar{y}_m \, dy \right]$$

$$+ \frac{2}{a} \left[\sum_{m=1}^{\infty} \frac{m\pi}{a} \frac{\sinh ((b-y)\gamma_m)}{\sinh b\gamma_m} \int_0^a \bar{T}_S \sin \bar{x}_m \, dx \right]$$

$$+ \frac{2}{a} \left[\sum_{m=1}^{\infty} \frac{m\pi}{a} \frac{\sinh \gamma_m y}{\sinh b\gamma_m} \int_0^a \bar{T}_N \sin \bar{x}_m \, dx \right] \qquad (32)$$

$$\phi_{x=a} = \frac{2}{b} \left[\sum_{m=1}^{\infty} \frac{m\pi}{b} \left\{ \sin \bar{y}_m \int_0^b \bar{T}_E \cos \bar{y}_m \, dy \right. \right.$$

$$\left. + \cos \bar{y}_m \int_0^b \bar{T}_E \sin \bar{y}_m \, dy \right\}$$

$$+ \sin \bar{y}_m \int_0^b \sin \bar{y}_m \frac{\partial T_E}{\partial y} dy \Bigg]$$

$$+ \frac{2}{b} \left[\sum_{m=1}^{\infty} \frac{\eta_m \sin \bar{y}_m}{\tanh a\eta_m} \int_0^b \bar{T}_E \sin \bar{y}_m \, dy \right]$$

$$+ \frac{2}{b} \left[\sum_{m=1}^{\infty} \frac{-\eta_m \sin \bar{y}_m}{\sinh a\eta_m} \int_0^b \bar{T}_W \sin \bar{y}_m \, dy \right]$$

$$+ \frac{2}{a} \left[\sum_{m=1}^{\infty} \frac{m\pi}{b} \frac{\sinh ((b-y)\gamma_m)}{\sinh b\gamma_m} (-1)^m \int_0^a \bar{T}_S \sin \bar{x}_m \, dx \right]$$

$$+ \frac{2}{a} \left[\sum_{m=1}^{\infty} \frac{m\pi}{a} \frac{\sinh \gamma_m y}{\sinh b\gamma_m} (-1)^m \int_0^a \bar{T}_N \sin \bar{x}_m \, dx \right] \qquad (33)$$

In Eqs. (30) through (33), the following abbreviations were used:

$$\begin{aligned} \bar{T}_N &= T_N(x) + \frac{a_2}{a_1} \\ \bar{T}_S &= T_S(x) + \frac{a_2}{a_1} \\ \bar{T}_E &= T_E(x) + \frac{a_2}{a_1} \\ \bar{T}_W &= T_W(x) + \frac{a_2}{a_1} \end{aligned} \qquad (34)$$

III. Summary

The purpose of this analysis is to determine the thermal influence of the antenna panels on the neighboring bars that make up the antenna backup structure. The problem analyzed is that of a flat rectangular plate under conductive, convective and radiative heat transfer. The plate is bounded by bars at its four edges. For arbitrary temperature boundary conditions we have determined the temperature distribution within the plate as well as the temperature flux at the edges. The analytical solutions are expressed in terms of trigonometric series. The panel heat fluxes at its edges represent, in turn, heat fluxes to or from the bars of the backup structure. Therefore, the interactions of fluxes obtained in this paper with fluxes from the bar model developed in Part I are necessary to develop the thermal behavior of the antenna reflector structure.

References

1. Schonfeld, D., and Lansing, F. L., "Thermal Analysis of Antenna Backup Structure, Part I—Methodology Development," *TDA Progress Report 42-70*, Jet Propulsion Laboratory, Pasadena, Calif., Aug. 15, 1982.

2. Polozhiy, G. N., *Equations of Mathematical Physics*, Hayden Book Co., N.Y., 1967, p. 404.

3. Carnahan, B., Luther, H. A., and Wilkes, J. O., *Applied Numerical Methods*, J. Wiley & Sons, N.Y., 1969.

4. Carslaw, H. S., and Jaeger, J. C., *Conduction of Heat in Solids*, Oxford University Press, 1959, p. 169.

List of Symbols

a	length of plate
a_1, a_2	coefficients in the generalized heat transfer equation
b	width of plate
F	radiation shape factor
h	heat transfer coefficient
I	solar radiation intensity
k	thermal conductivity
T	absolute temperature
α	solar radiative absorptance
ϵ	radiative emittance
σ	Stefan-Boltzman constant
ϕ	Flux from the edge of the plate

Subscripts

a	ambient
c	convective
r	radiative

Table 1. Comparison of numerical and series results for conduction heat transfer only

y/b	Temperature map in the plate–series solution, x/a = 0.0	0.1	0.2	0.3	0.4	0.5	0.6	0.7	0.8	0.9	1.0
1.0	50.00	65.00	80.00	95.00	110.00	125.00	140.00	155.00	170.00	185.00	200.00
0.9	75.00	87.31	98.04	109.93	120.90	133.02	143.93	156.49	167.35	181.31	190.00
0.8	100.00	108.64	116.43	124.32	132.28	140.36	148.50	156.85	165.52	174.93	180.00
0.7	125.00	130.31	134.41	138.83	143.34	147.91	152.56	157.34	162.32	167.90	170.00
0.6	150.00	150.84	152.26	153.29	154.32	155.39	156.50	157.65	158.77	159.23	160.00
0.5	175.00	173.05	170.20	167.72	165.27	162.82	160.39	157.95	155.46	153.20	150.00
0.4	200.00	193.52	188.09	182.16	176.20	170.24	164.28	158.29	152.25	145.80	140.00
0.3	225.00	216.21	206.08	196.60	187.14	177.67	168.18	158.68	149.16	139.94	130.00
0.2	250.00	236.08	223.95	211.07	198.06	185.12	172.09	159.11	146.05	132.66	120.00
0.1	275.00	260.22	241.06	226.23	208.45	193.04	175.61	159.96	142.61	127.18	110.00
0.0	300.00	280.00	260.00	240.00	220.00	200.00	180.00	160.00	140.00	120.00	100.00

y/b	Temperature map in the plate–numerical solution, x/a = 0.0	0.1	0.2	0.3	0.4	0.5	0.6	0.7	0.8	0.9	1.0
1.0	50.00	65.00	80.00	95.00	110.00	125.00	140.00	155.00	170.00	185.00	200.00
0.9	75.00	87.63	99.72	111.53	123.15	134.65	146.02	157.28	168.40	179.34	190.00
0.8	100.00	109.68	118.69	127.26	135.53	143.57	151.39	158.99	166.34	173.38	180.00
0.7	125.00	131.41	137.15	142.42	147.32	151.91	156.22	160.25	163.94	167.22	170.00
0.6	150.00	152.94	155.28	157.15	158.64	159.80	160.64	161.14	161.26	160.92	160.00
0.5	175.00	174.33	173.15	171.55	169.59	167.31	164.70	161.73	158.36	154.49	150.00
0.4	200.00	195.62	190.83	185.69	180.24	174.49	168.44	162.05	155.26	147.95	140.00
0.3	225.00	216.82	208.34	199.60	190.61	181.38	171.89	162.10	151.94	141.30	130.00
0.2	250.00	237.94	225.70	213.28	200.70	187.95	175.00	161.83	148.37	134.49	120.00
0.1	275.00	259.00	242.92	226.76	210.51	194.17	177.73	161.17	144.44	127.45	110.00
0.0	300.00	280.00	260.00	240.00	220.00	200.00	180.00	160.00	140.00	120.00	100.00

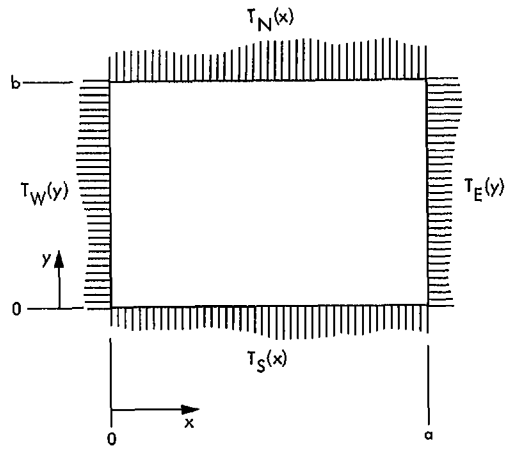

Fig. 1. Geometry of panel analyzed

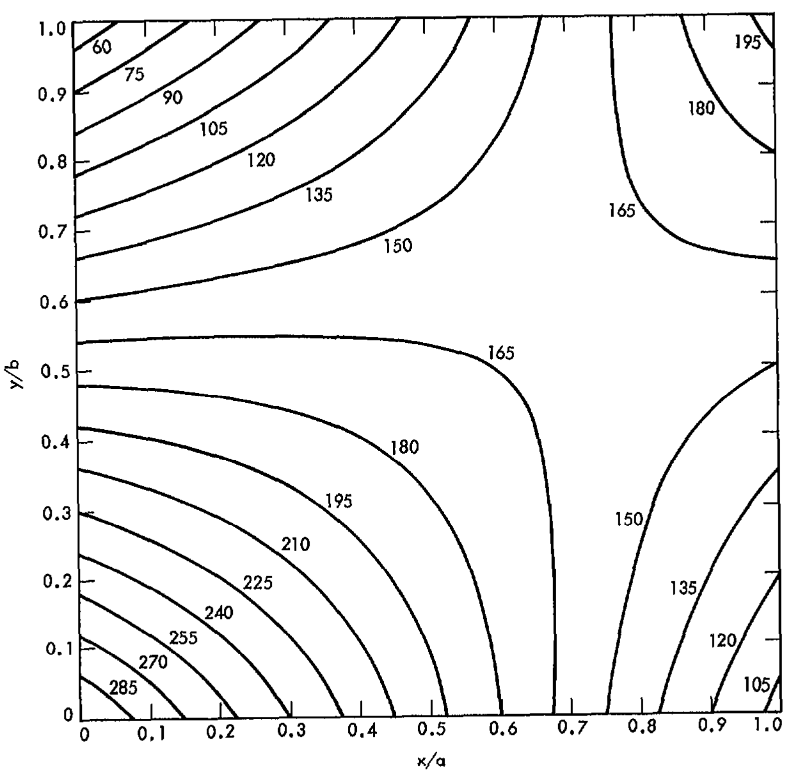

Fig. 2. Isotherms in a plate with conduction heat transfer only

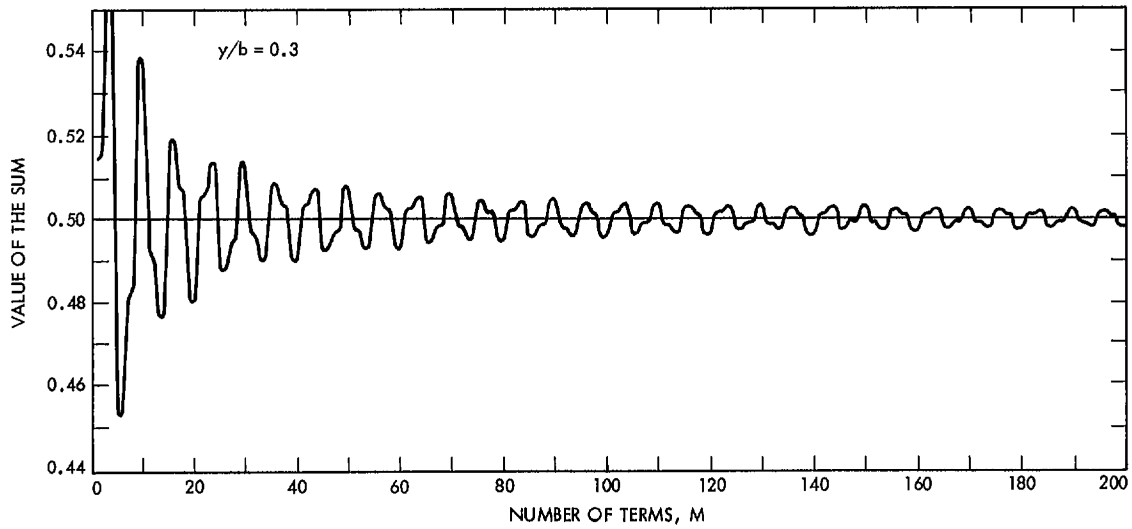

Fig. 3. Series convergence for $y/b = 0.3$

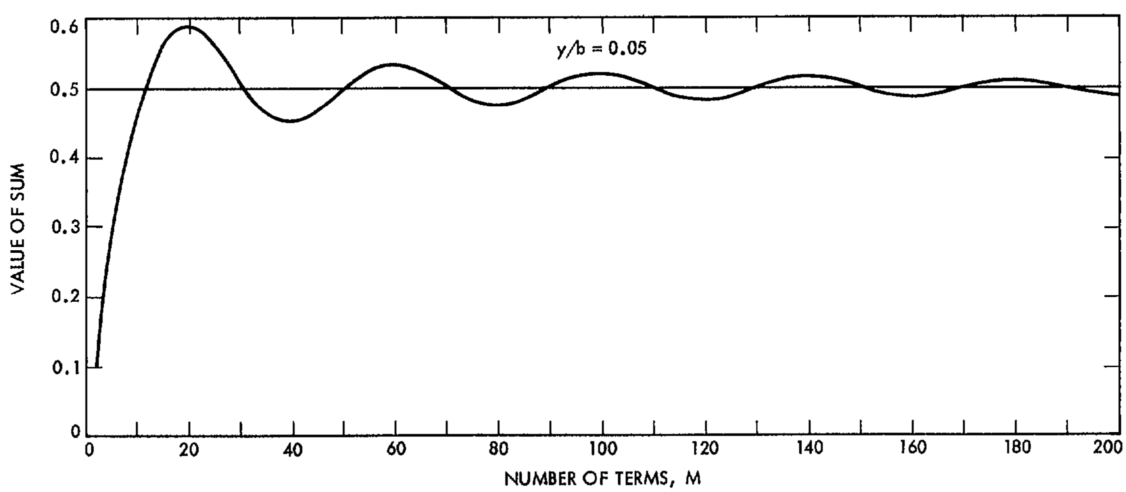

Fig. 4. Series convergence for $y/b = 0.05$